HHS Public Access

Author manuscript

Cell Rep. Author manuscript; available in PMC 2016 July 07.

Published in final edited form as:

Cell Rep. 2016 June 28; 16(1): 9–18. doi:10.1016/j.celrep.2016.05.086.

Cholesterol-independent SREBP-1 maturation is linked to ARF1 inactivation

Lorissa J. Smulan[1], **Wei Ding**[1], **Elizaveta Freinkman**[2], **Sharvari Gujja**[1], **Yvonne J. K. Edwards**[1], and **Amy Walker**[1]

[1]Program in Molecular Medicine, UMASS Medical School, 373 Plantation Street, Worcester, MA 01605

[2]Metabolite Profiling Facility, Whitehead Institute for Biomedical Research, 9 Cambridge Center, Cambridge, MA 02142

Summary

Lipogenesis requires coordinated expression of genes for fatty acid, phospholipid, and triglyceride synthesis. Transcription factors, such as SREBP-1 (Sterol regulatory element binding protein), may be activated in response to feedback mechanisms linking gene activation to levels of metabolites in the pathways. SREBPs can be regulated in response to membrane cholesterol and we also found that low levels of phosphatidylcholine (a methylated phospholipid) led to SBP-1/SREBP-1 maturation in *C. elegans* or mammalian models. To identify additional regulatory components, we performed a targeted RNAi screen in *C. elegans*, finding that both *lpin-1/Lipin 1* (converts phosphatidic acid to diacylglycerol) and *arf-1.2/ARF1* (a GTPase regulating Golgi function) were important for low-PC activation of SBP-1/SREBP-1. Mechanistically linking the major hits of our screen, we find that limiting PC synthesis or *LPIN1* knockdown in mammalian cells reduces levels of active GTP-bound ARF1. Thus, changes in distinct lipid ratios may converge on ARF1 to increase SBP-1/SREBP-1 activity.

Graphical Abstract

corresponding author amy.walker@umassmed.edu.

CrediT Taxonomy

Conceptualization and Methodology A.K.W; Software, S.G., Y.J.K.E.; Validation, L.J.S, W.D., A.K.W.; Formal Analysis, L.J.S., A.K.W.; Investigation, L.J.S., W.D., A.K.W.; Writing-original draft, Writing-reviewing and editing, Visualization, Supervision, Project Administration and Funding Acquisition, A.K.W.

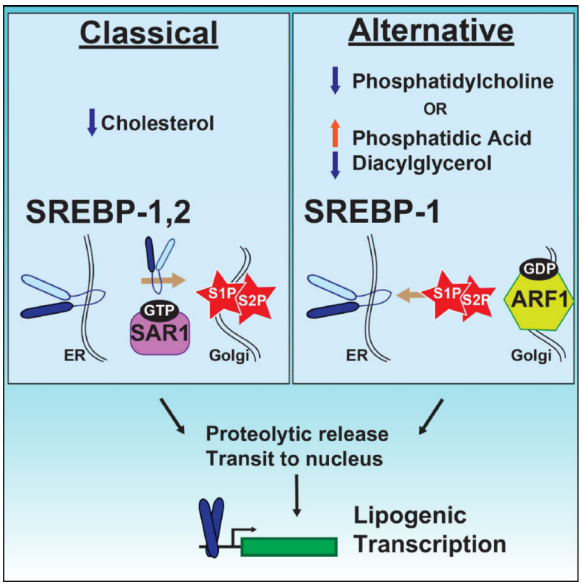

Introduction

Metabolic gene regulation is often connected to products or substrates in the pathway. In some cases, such as low-cholesterol stimulated maturation of SREBP (Sterol regulatory element binding protein) transcription factors, mechanisms have been described in detail. SREBPs reside in the endoplasmic reticulum (ER) as membrane intrinsic, inactive precursors (Osborne and Espenshade, 2009). Drops in intramembrane cholesterol promote transport of SREPB to the Golgi (Goldstein et al., 2006) where proteases release the transcriptionally active portion (Brown and Goldstein, 1997). SREBPs regulate genes required for fatty acid, TAG (triglyceride), PC (phosphatidylcholine) and cholesterol synthesis (Horton et al., 2002), therefore, it is not surprising that control of SREBP activity is complex and responds to a variety of metabolic signals. SREBP-2 is tightly linked to cholesterol synthesis, whereas the SREBP-1a/c isoforms have a broader roles (Horton, 2002). Using *C. elegans* and mammalian models, we previously found that low levels of SAM acted through PC to induce cholesterol-independent SREBP-1 processing (Walker et al., 2011). Instead of depending on COP II transit to the ER, low PC was associated with dissolution of Golgi markers, suggesting SREBP-activating proteases may cleave ER bound SREBP-1, as in Brefeldin-A mediated activation (DeBose-Boyd et al., 1999). However, regulatory factors linking PC to these processes were unclear.

To identify additional factors in this pathway, we performed a *C. elegans* RNAi screen using the SBP-1/SREBP-1 responsive reporter. Our genetic approach identified *lpin1/LPIN1* and *arf-1.2/ARF1*, suggesting that like cholesterol-dependent regulation of SREBP-2, low-PC effects on SREBP-1 are linked to effects of membrane lipids on intracellular transport, however in this case, intermediates in the TAG/PC synthesis pathway, such as PA and DAG, may affect Golgi to ER COP I function.

Results

Targeted RNAi screen to reveal low-PC modulators of SBP-1

To identify components in low-PC activation of SBP-1/SREBP-1, we performed a targeted RNAi screen comparing activation of a SBP-1-dependent reporter, *pfat-7*::GFP, in wild type and low-PC conditions. *fat-7* encodes a stearoyl-CoA desaturase (SCD) regulated by SBP-1 (Yang et al., 2006). Depletion of PC synthesis enzymes (*sams-1, pmt-1, cept-1, pcyt-1*), stimulates SBP-1 and *fat-7* levels increase (Walker et al., 2011) (Figure 1A). We focused on metabolic pathways producing or utilizing PC, genes involved in lipid-based signaling, and a subset of genes linked to COP I or II transport. Next, we selected an RNAi sublibrary from the ORFeome collection (Rual et al., 2004), the Ahringer library (Kamath et al., 2003), or constructed RNAi targeting vectors (Table S1). We screened for candidates satisfying two criteria: first, necessary for *pfat-7*::GFP induction in low-PC *sams-1(lof)* animals, and second, sufficient to activate *pfat-7*::GFP in wild type phospholipid levels (Figure 1B).

We screened four library replicates and divided candidates into four classes according to GFP expression and genotype (Figure 1B; Table S1). Class 1 or class 2 genes limited or increased *pfat-7*::GFP expression and comprised 49(23%) or 10(5%) of clones screened. Candidate class 3 genes were associated with decreases in *sams1(lof); pfat-7*::GFP (68 genes) and there were no genes that increased *pfat-7*::GFP in *sams-1(lof)* animals (class 4). Class 1 and class 3 genes are predicted to be generally important for SBP-1 function, and indeed include many regulators of classical SREBP-1 processing such as *scp-1* (SCAP, SREBP cleavage-activating protein), and the COP II components such as *sec-23, sec-24.1* and *sar-1* (Figure 1C, **red lettering**). As in our previous data, PC synthesis genes (*pcyt-1* and *cept-1*) (Figure 1D, **red labeling**) fell into class 2 (Walker, et al., 2011). Genes necessary for low-PC processing and sufficient to activate SBP-1 in normal PC (Figure 1D, **red lettering**) were predicted to lie in the intersection of candidate classes 2 and 3. The GTPase *arf-1.2* was present in this category, as well a phospholipase C ortholog. However, the PA phosphatase *lpin-1* (Reue, 2007) showed the most striking increase in *pfat-7*::GFP combined with decrease in *sams-1(lof);pfat-7*::GFP (Figure 1D–G Table S1).

Next, we used quantitative RT-PCR (qRT-PCR) to determine expression of *gfp*, endogenous *fat-7* and *fat-5* (another SBP-1 responsive gene) in the reporter strain and also analyzed *fat-7* and *fat-5* expression in wild type animals. First, we confirmed that 5 of the top 10 class 1 genes were necessary for *pfat-7*::GFP mRNA expression (see Table S1; **see column K–M for validation**). For class 2 genes, we found that only *lpin-1, arf-1.2* and *plc-1* RNAi increased *gfp*, endogenous *fat-7* and *fat-5* mRNA levels (Figure S1B, D). *lpin-1, arf-1.2* and *plc-1* RNAi also decreased *gfp* levels in the low-PC *sams-1(lof);pfat-7*::GFP (Figure S1C, E). Finally, while *lpin-1* and *arf-1.2* RNAi increased endogenous *fat-7* and *fat-5* in wild type worms, *plc-1* effects occurred only in the transgenic strain (Figure S1D). We also noted that *sams-1(lof)* animals with reduced *lpin-1* showed additional phenotypes, including slowed development and synthetic lethality (Figure S1G).

The importance of *lpin-1* for low-PC activation *pfat-7*::GFP prompted us to examine pathways producing the LPIN-1 substrate, PA. *C. elegans* contains multiple paralogs of PA synthesis genes (Figure S1A): three GPATs, *acl-4, -5* and *-6* and two AGPATs, *acl-11* and

acl-13 (Ohba et al., 2013). Our screen data showed that one GPAT (*acl-4*) and one AGPAT (*acl-11*) were required for *pfat-7*::GFP expression in wild type, but not in *sams-1(lof)* animals (Figure 1C). In validation assays, we found GFP was lower after *acl-4* or *acl-11* RNAi (Figure S2A), as were *gfp* and endogenous *fat-7* mRNA levels (Figure S2B). *pfat7::gfp* or endogenous *fat-7* gene expression was not altered by *acl-4* and *acl-11* RNAi in low-PC (*sams-1(lof); pfat-7*::GFP) conditions (Figure S2C, D).

sams-1 or *lpin-1* RNAi reduce DAG and change PA/PC ratios in *C. elegans* microsomal membranes

Loss of *sams-1* decreases PC and increases TAG (Ding et al., 2015; Walker et al., 2011), however, *lpin-1* knockdown is predicted to affect PA and DAG (Figure S1A). To generate lipid profiles in membranes linked to SBP-1/SREBP-1 processing, we profiled microsomal lipids from *sams-1* or *lpin-1* RNAi animals. We validated fractionations by immunobloting with *C. elegans* ER or Golgi specific antibodies (Figure S3A). LC/MS analysis identified over 1600 lipid species in over 20 classes (Table S2). Principal component analysis shows that control, *sams-1* and *lpin-1* RNAi samples are distinct and that biological replicates are similar (Figure S3B). We analyzed the data in two ways: first, values for lipid species were totaled for each class and second, the distribution of species within each class was determined. In *sams-1(RNAi)* microsomal fractions, we found that TAGs as a class were increased and PCs as a class were decreased (Figure S2 C, D; see Table S2 **for statistics**), as in our previous studies analyzing whole worm extracts by GC/MS (Ding et al., 2015; Walker et al., 2011). Many other lipid species also changed (Figure S3E, Table S2), perhaps in response to synthetic links between PC and other lipids. We were surprised to see that DAG as a class was similar to wild type, however, many individual species shifted significantly lower and the distribution of species within the class differed significantly after *sams1(RNAi)* (Figure S3F, Table S2). This is in contrast to models for PC metabolism that predict increased DAG when PC synthesis is blocked (Sarri et al., 2011) and may reflect the specific nature of our assay.

lpin-1 RNAi, on the other hand, had fewer overall effects, primarily lowering levels of many DAG species and increasing multiple PA species (Figure S3F–I, see Table S2 **for statistics**), consistent with a role for *lpin-1* as a PA phosphatase. Finally, we noted two major similarities in *sams-1* and *lpin-1* lipid profiles. First, ratios of PA/PC species were elevated, and second, the distribution of species within the DAG class shifted significantly lower. This is consistent with our genetic evidence implicating enzymes directly liked to PA, DAG, and PC in the regulation of *pfat-7*::GFP.

lpin-1 and *arf-1.2* are important for low-PC effects on SBP-1

Increased *fat-7* expression after *lpin-1 RNAi* suggests SBP-1 may be more active. To determine if maturation was stimulated, we examined subcellular localization of intestinal GFP::SBP-1 (Walker et al., 2010). Similar to *sams-1* RNAi, knockdown of either *lpin-1* or *arf-1.2* resulted in increased nuclear levels of GFP::SBP-1 (Figure 2A), along with increases in *fat-7* and *fat-5* (Figure 2B). Interestingly, we noted that *lpin-1* expression was slightly increased after *sams-1* RNAi (Figure 2B); see also (Ding et al., 2015). Finally, depletion of

PA synthesis enzymes *acl-4* and *acl-11* had opposite effects, decreasing nuclear SBP-1 (Figure S2E–G)

Next, we performed Sudan Black staining to gauge size and distribution of lipid droplets and measured TAG for total levels. To avoid confounding results from the developmental delay of *sams-1(lof); lpin-1(RNAi)* animals (Figure S1G), PC production was rescued with choline until the L3 stage (Ding, et al 2015); growth without choline after L3 was sufficient to increase SBP-1-dependent gene expression (Figure S1H). *lpin-1* RNAi animals appeared clear with slightly reduced Sudan Black staining (Figure 2C, D), consistent with reports of decreased Nile Red (Golden et al., 2009; Zhang et al., 2013), however TAG stores were not reduced in colorometric assays (Figure 2E) or microsomal extracts (Table S2, **see tab:TG.class**). This suggests other mechanisms may compensate for LPIN-1 function in TAG synthesis. Importantly, large lipid droplets in *sams-1(lof)* animals decreased upon *lpin-1* RNAi and TAG returned close to wild type levels (Figure 2C–E). Thus, interference with both *sams-1* and *lpin-1* rescues effects of low-PC on stored lipids.

arf-1.2 knockdown also increased *fat-7* expression and nuclear localization of GFP::SBP-1 (Figure 2A, B). Therefore, we assessed Sudan Black staining and TAG levels. *arf-1.2(RNAi)* worms had an increase in lipid droplets (Figure 2F, G), however, TAG levels were only slightly higher than wild type (Figure 2H), suggesting effects on droplets size and not total lipid levels. This is consistent with reports of ARF function in lipid droplet formation (Wilfling et al., 2014). In contrast, *arf-1.2 RNAi* reduced lipid droplet appearance, number and overall TAG levels in *sams-1(lof)* animals. Taken together, our *C. elegans* studies show that reducing function of LPIN-1, an enzyme converting PA to DAG, limits low-PC activation of SBP-1/SREBP. Thus, enzymes that produce or utilize PA may be a key to this mechanism.

LPIN1 knockdown is sufficient to activate mammalian SREBP-1 and necessary for low-PC effect

In mammals, interference with PC synthesis results in hepatosteatosis (Vance, 2014), as SREBP-1-dependent lipogenesis programs are stimulated (Walker et al., 2011). To determine if Lipin 1 was required for activation of mammalian SREBP-1 in this context, we depleted *LPIN1* with siRNA. Like knockdown of *PCTY1a*/CCTa, the rate limiting enzyme in mammalian PC production, *LPIN1* depletion increased levels of mature, nuclear SREBP-1 (Figure 3A–C). *LPIN1* knockdown also increased nuclear localization and proteolytic maturation of a N-terminal HA tagged SREBP-1 (Figure 3D; Figure S4A, B). siRNA-mediated depletion was confirmed by qRT-PCR and immunoblots from Dignam extracts of HepG2 cells (Figure S4C, D).

To determine if *LPIN1* function was important for low-PC effects on SREBP-1, we used siRNA to deplete both *PCTY1a* and *LPIN1* in HA-SREBP-1 lines. For combined siRNA, we kept RNA amounts constant with scrambled control and achieved efficient knockdown for both *PCTY1a* and *LPIN1* (Figure S4C). We found that nuclear HA-SREBP-1 localization was lost in *PCTY1a*/LPIN1 double knockdowns (Figure 3D, F), suggesting that as in *C. elegans, LPIN1* knockdown abrogates the low-PC effect on SREBP-1. Similar effects were seen with endogenous SREBP-1 (Figure S4E, F).

Lipin 1 converts PA to DAG, thus lower activity predicts increases in PA (Takeuchi and Reue, 2009). To determine if exogenous PA could recapitulate *LPIN1*effects, we treated HA-SREBP-1 cells with PA and found that indeed, SREBP-1 nuclear accumulation increased (Figure 3E, G). Further paralleling *LPIN1* knockdown, PA decreased nuclear SREBP-1 in *PCTY1a* siRNA cells (Figure 3E, G). Although effects of exogenous PA on cultured cells may be complex and have species dependent effects, changes in SREBP-1 maturation are consistent with effects of *LPIN1* knockdown. We also investigated low-PC induced lipid droplet formation and found that, as in *C. elegans*, co-depletion of *PCTY1a* with *LPIN1* restored lipid droplets to wild type levels (Figure S4G–I). Taken together, our results suggest that inhibiting *LPIN1* expression or adding its exogenous substrate can reverse the effects of *PCYT1a* knockdown on SREBP-1.

Lipin 1 has been shown to inhibit SREBP-1 activity when mTORC1-dependent (mechanistic Target of Rapamycin Complex) phosphorylation decreases and it localizes to the nucleus, sequestering SREBP-1 at the nuclear membrane. However, mechanisms linking low-PC SREBP-1 activation to Lipin 1 appear distinct. First, SREBP-1 nuclear localization after *PCTY1A* or *LPIN1* knockdown is nucleoplasmic and target genes are activated (see also (Walker et al., 2011)). Second, localization of endogenous Lipin 1(Figure S5A, B; specificity antibody shown in Figure S5C), or a transfected Flag-Lipin 1 (Figure S5D) is not changed after *PCTY1A* knockdown. Finally, fractionation experiments show similar levels of Lipin 1 isoforms in nuclear/ER and microsomal fractions in control and *PCTY1a* extracts (Figure S5E). Lipin 1 may also act in co-activation of β-oxidation genes (Reue and Zhang, 2008), however, these genes are not altered upon *PCYT1a* depletion (Figure S5F). Thus, mechanisms linking Lipin 1 and SREBP-1 in low PC appear distinct from mTORC1-mediated control of Lipin 1 localization or direct effects on gene regulation.

PCTY1a and *LPIN1* knockdown affect ARF1 activity

Our previous studies found that low-PC or disruptions in ARF1 GEF(Guanine Exchange Factor) GBF1 induced maturation of SREBP-1 (Walker et al., 2011) and our *C. elegans* screen also implicated *arf-1.2* in SBP-1 activation (Figure 1D, F; Figure 2A). To determine if this mechanism extended to mammalian cells, we examined SREBP-1 localization and processing in HepG2 cells after ARF1 siRNA and found that nuclear accumulation increased and processed SREBP-1 appeared at higher levels (Figure 3H–J).

The validated hits from our *C. elegans* screen strongly implicated enzymes that alter PA or DAG levels in low-PC mediated processing of SREBP-1. Interestingly, both PA and DAG have been reported to affect ARF1 function, interfering with COP I transport (Asp et al., 2009; Fernandez-Ulibarri et al., 2007; Manifava et al., 2001). Therefore, we asked if knockdown of *LPIN1* or *PCYT1a* affected levels of active, GTP-bound ARF1 and found that, strikingly, levels were diminished in both instances (Figure 4A–C). As in our previous assays, double knockdown of *LPIN1* and *PCYT1a* corrected defects (Figure 4D, E). Finally, we asked if exogenous PA would phenocopy *LPIN1* knockdown and rescue *siPCYT1a* effects on GTP-ARF levels and found partial rescue of active ARF1 (Figure 4F, G).

Cytosolic membrane levels of PA (Csaki et al., 2014), DAG (Sarri et al., 2011), or PC (Vance, 2014) could be affected in either *LPIN1* or *PCYT1a* knockdown. Interestingly,

ARF1 activity depends on membrane recruitment of the GTPase itself along with membrane association of the GAP (GTPase Activating Protein, ARFGAP1) and GEF (GBF1) (Bankaitis et al., 2012; Lev, 2006; Spang, 2002). In addition, DAG levels may be important for ARFGAP1 association (Antonny et al., 1997; Bigay et al., 2003; Fernandez-Ulibarri et al., 2007). Therefore, we compared association of ARF1, GBF1 or ARFGAP1 with microsomal membranes after *PCYT1*a or *LPIN1* siRNA. Strikingly, GBF1 association was broadly decreased, while ARFGAP1 and ARF1 did not change (Figure 4 H, I; Figure S5G, H). This suggests that local changes in membrane lipids occurring after *PCYT1a* or *LPIN1* depletion may have profound effects on recruitment GBF1, leading to disruptions in ARF1 activity activating SREBP-1.

Discussion

Lipid storage requires coordinated production of fatty acids, phospholipids, TAGs and other complex lipids (Horton et al., 2002). Many of these lipids also function in membrane structure or as signaling effectors, thus regulators of lipogenesis may respond to various signals. Our screen identified *lpin-1*, a PA phosphatase, (Takeuchi and Reue, 2009) as an activator of SBP-1/SREBP-1. Although enzymatic activities of lipins suggest straightforward synthetic functions, they have diverse roles and broad physiological effects (Csaki et al., 2014). For example, the *fld* mouse model of *LPIN1* deficiency has metabolic defects including fatty liver and lipodystrophy (Peterfy et al., 2001) and the SREBP-1 transcriptional target SCD1 is upregulated (Chen et al., 2008). Lipin 1 has also been reported to affect SREBP-1 activity through nuclear membrane sequestration (Peterson et al., 2011) or to act as a co-activator of β-oxidation genes with PPARα (Finck et al., 2006); however, neither of these activities was altered after *PCYT1/CCTa* knockdown. In this context, we hypothesize Lipin 1-dependent effects on SREBP-1 occur when changes in changes membrane lipids alter membrane:protein interactions and activity of GBF-1 and ARF-1.

Changes in PA, DAG, or PC within subcellular membranes could have multiple effects. However, our data suggested a connection to ARFs. Notably, several studies have found that DAGs are important for ARF1 function or for recruiting ARFGAP (Antonny et al., 1997; Bigay et al., 2003; Fernandez-Ulibarri et al., 2007; Randazzo and Kahn, 1994). However, we found that it was the ARF-GEF, GBF1, that bound less well to membranes after *PCYT1* or *LPIN1* knock down. Loss of GBF1 activates the unfolded protein response and promotes cell death in mammalian cells (Citterio et al., 2008), and defects in development and Golgi integrity in *C. elegans* (Ackema et al., 2013). However, larval growth arrest after *gbf-1(RNAi)* in our screen precluded analysis. A recent study has suggested that GBF1 is recruited to membranes in response to increases in ARF-GDP (Quilty et al., 2014). We hypothesize that local changes in ratios of PA to PC species or decreases in DAG species, as seen in our studies of *C. elegans* microsomes, limit GBF1 recruitment and prevent generation of GTP-bound ARF1. In this instance, there could be insufficient DAG for recruitment or changes in curvature predicted by a PA-rich membrane could disrupt membrane:protein interactions.

Finally, we have found that co-depletion of PC biosynthetic enzymes and *lpin-1*/LPIN1 returns SBP-1/SREBP-1 function to basal levels and restores TAG levels. In this case,

inhibiting the PA to DAG transition could limit both TAG and PC. We hypothesize this allows levels to rebalance, restoring ARF1 function and baseline SBP-1/SREBP-1 activity. Thus, our results suggest SBP-1/SREBP-1 transcriptional programs favoring lipogenesis may be stimulated when the balance of PA, DAG or PC change within microsomal membranes.

Experimental Procedures

C. elegans: strains and RNAi constructs

Nematodes were cultured using standard *C. elegans* methods. For information on strains and RNAi constructs, see Table S2.

C. elegans: RNAi screen

L1 larva were plated into 96 well plates arrayed with RNAi bacteria and scored at the L4/young adult transition. Each well was given a score from −3 to +3 with 0 as no change in 4 independent replicates and scores were averaged. RNAi clones whose average scores were >0.7 or <−0.7 were selected as candidates for validation.

C. elegans: GFP visualization

pfat-7::GFP and SBP-1::GFP *C. elegans* strains were grown until the L4/young adult transition and images were acquired on a Leica SPE II confocal microscope. All images were taken at identical gain settings within experimental sets and Adobe Photoshop was used for corrections to levels across experimental sets.

C. elegans: Gene Expression Analysis

C. elegans at the L4/young adult transition were lysed and qRT-PCR analysis was performed as in Ding et al. 2015. Primers are available upon request.

C. Elegans: Lipid Analysis

C. elegans were grown on plates containing 30 mM choline until L2, washed, and transferred to plates without cholineuntil the second day of adulthood. Sudan Black staining was performed as in Ding, et al. 2015. Briefly, animals were dehydrated in ethanol, stained with Sudan Black, placed on agar pads and photographed in bright field microscopy with a Leica SPE II. Sudan Black staining was quantitated by blind scoring of more then 30 for of small, medium, or large lipid droplets. TAG levels were determined using a Triglyceride Colorimetric Assay Kit (Cayman Chemical, 10010303) following manufacturer's instructions. For quantitation of TAG levels, 2-tailed Students T tests were used to determine significance between three biological replicates. For lipidomic methods, see Supplemental methods.

Cell Culture: Media and Stable Cell Lines

HepG2 cells (ATCC, HB-8065) were maintained in Minimum Essential Medium (Invitrogen) supplemented with 10% FBS (Invitrogen), Glutamine (Invitrogen), and Sodium Pyruvate (Invitrogen). HepG2 cells stably expressing human SREBP-1c were generated by

transfection of a pCMV6 SREBP-1c with an N-terminal hemagglutinin (HA) epitope tag (Origene, RC208404) and selection with Geneticin (Invitrogen).

Cell Culture: Transfection and siRNA

siRNA oligonucleotides were transfected for 48 hours with Lipofectamine RNAiMAX Transfection Reagent (Invitrogen, 13778100) (see Table S2 for specific siRNAs). Cells were incubated for 16 hours in 1% Lipoprotein Deficient Serum (LDS) (Biomedical Technologies, BT907) and 25 μg/ml ALLN (Calbiochem) for 30 min prior to harvesting. For studies with co-depletion of *PCYT1a* and *LPIN1*, equal amounts of each siRNA or targeting plus scrambled were transfected.

Cell Culture: Gene Expression

Total mRNA was extracted from with Tri-Reagent according to manufacturer's protocol (Sigma). qRT-PCR conditions were identical to *C. elegans* studies. For qRT-PCR studies, graphs represent representative experiments selected from at least three biological replicates. 2-tailed Students T-tests were used to compare significance between values with two technical replicates. Primer sequences are available upon request.

Lipid Vesicle formation

Lipid vesicles containing 1,2-dipalmitoyl-*sn*-glycero-3-phosphate (PA) (Avanti Polar Lipids, 830855P) were prepared by water bath sonication as in (Zhang et al., 2012) and added at final concentrations of 100 μM during the 16 hour incubation in 1% LDS.

Immunofluorescence and Oil Red O staining

Transfected cells were fixed in 3.7% paraformaldehyde and permeabilized in 0.5% NP-40 prior before blocking in 5% fetal bovine serum/ 0.1% NP-40 and antibody treatment. For Oil Red O, cells were fixed with 3.7% paraformaldehyde, stained with Oil Red O (3mg/ml in 60% isopropanol) for 10 min and visualized. For quantification of antibody staining or lipid droplets, 10 individual focal areas were photographed, then scored blind for high, medium or low nuclear accumulation (antibody) or analyzed using BioPix iQ 2.1.4 (droplets). 2-tailed Students T tests were used to compare significance between the 10 photograhed areas and are representative of three biological replicates. All images within experimental sets were taken with a Leica SPE II at identical confocal gain settings and Adobe Photoshop was used for levels corrections.

Immunoblot Analysis

Cells were lysed by syringe in High Salt RIPA (50 mM Tris, pH 7.4; 400 mM NaCl; 0.1% SDS; 0.5% NaDeoxycholate; 1% NP-40; 1 mM DTT, 2.5 μg/mL ALLN, Complete protease inhibitors (Roche). Extracts were separated on Invitrogen NuPage gels (4–12%), transferred to nitrocellulose and probed with specified antibodies. Immune complexes were visualized with Luminol Reagent (Millipore). Densitometry was performed by scanning of the film, then analysis of pixel intensity with ImageJ software. Graphs show average of at least three independent experiments with control values normalized to one.

Cell Fractionation: HepG2

Transfected cells were resuspended in cold homogenization buffer (Microsome purification kit, Biovision) and dounced, then cleared briefly. Supernatants were centrifuged at 80,000g for 45 minutes. Pellets were collected as microsomal fractions with the supernatant designated as the cytosolic fraction.

Active Arf1 Analysis

Levels of active Arf1 were analyzed using an Active Arf1 Pull-Down and Detection Kit (ThermoSCIENTIFIC) following manufacturer's instructions. Densitometry was performed by scanning of the film, then analysis of pixel intensity with ImageJ software. Graphs show average of at least three independent experiments with control values normalized to one.

Supplementary Material

Refer to Web version on PubMed Central for supplementary material.

Acknowledgments

We thank Drs. David Lambright and Stefan Taubert for reading of the manuscript as well as Drs. Marian Walhout (UMASS Medical School), Victor Ambros (UMASS Medical School), Michael Czech (UMASS Medical School), Michelle Mondoux (College of the Holy Cross) and members of their labs for helpful discussion. We also thank Dr. Michael Lee (UMASS) for advice on bioinformatics. Some *C. elegans* strains were provided by the *Caenorhabditis* Genetics Center (CGC), which is funded by NIH Office of Research Infrastructure Programs (P40 OD010440). This work was supported by the NIH through R01DK084352 to A.K.W.

References

Ackema KB, Sauder U, Solinger JA, Spang A. The ArfGEF GBF-1 Is Required for ER Structure, Secretion and Endocytic Transport in. PloS one. 2013; 8:e67076. [PubMed: 23840591]

Antonny B, Huber I, Paris S, Chabre M, Cassel D. Activation of ADP-ribosylation factor 1 GTPase-activating protein by phosphatidylcholine-derived diacylglycerols. J Biol Chem. 1997; 272:30848–30851. [PubMed: 9388229]

Asp L, Kartberg F, Fernandez-Rodriguez J, Smedh M, Elsner M, Laporte F, Barcena M, Jansen KA, Valentijn JA, Koster AJ, et al. Early stages of Golgi vesicle and tubule formation require diacylglycerol. Mol Biol Cell. 2009; 20:780–790. [PubMed: 19037109]

Bankaitis VA, Garcia-Mata R, Mousley CJ. Golgi membrane dynamics and lipid metabolism. Curr Biol. 2012; 22:R414–R424. [PubMed: 22625862]

Bigay J, Gounon P, Robineau S, Antonny B. Lipid packing sensed by ArfGAP1 couples COPI coat disassembly to membrane bilayer curvature. Nature. 2003; 426:563–566. [PubMed: 14654841]

Brown MS, Goldstein JL. The SREBP pathway: regulation of cholesterol metabolism by proteolysis of a membrane-bound transcription factor. Cell. 1997; 89:331–340. [PubMed: 9150132]

Chen Z, Gropler MC, Norris J, Lawrence JC Jr, Harris TE, Finck BN. Alterations in hepatic metabolism in fld mice reveal a role for lipin 1 in regulating VLDL-triacylglyceride secretion. Arterioscler Thromb Vasc Biol. 2008; 28:1738–1744. [PubMed: 18669885]

Citterio C, Vichi A, Pacheco-Rodriguez G, Aponte AM, Moss J, Vaughan M. Unfolded protein response and cell death after depletion of brefeldin A-inhibited guanine nucleotide-exchange protein GBF1. Proc Natl Acad Sci U S A. 2008; 105:2877–2882. [PubMed: 18287014]

Csaki LS, Dwyer JR, Li X, Nguyen MH, Dewald J, Brindley DN, Lusis AJ, Yoshinaga Y, de Jong P, Fong L, et al. Lipin-1 and lipin-3 together determine adiposity in vivo. Mol Metab. 2014; 3:145–154. [PubMed: 24634820]

DeBose-Boyd RA, Brown MS, Li WP, Nohturfft A, Goldstein JL, Espenshade PJ. Transport-dependent proteolysis of SREBP: relocation of site-1 protease from Golgi to ER obviates the need for SREBP transport to Golgi. Cell. 1999; 99:703–712. [PubMed: 10619424]

Ding W, Smulan LJ, Hou NS, Taubert S, Watts JL, Walker AK. s-Adenosylmethionine Levels Govern Innate Immunity through Distinct Methylation-Dependent Pathways. Cell Metab. 2015

Fernandez-Ulibarri I, Vilella M, Lazaro-Dieguez F, Sarri E, Martinez SE, Jimenez N, Claro E, Merida I, Burger KN, Egea G. Diacylglycerol is required for the formation of COPI vesicles in the Golgi-to-ER transport pathway. Mol Biol Cell. 2007; 18:3250–3263. [PubMed: 17567948]

Finck BN, Gropler MC, Chen Z, Leone TC, Croce MA, Harris TE, Lawrence JC Jr, Kelly DP. Lipin 1 is an inducible amplifier of the hepatic PGC-1alpha/PPARalpha regulatory pathway. Cell Metab. 2006; 4:199–210. [PubMed: 16950137]

Golden A, Liu J, Cohen-Fix O. Inactivation of the *C. elegans* lipin homolog leads to ER disorganization and to defects in the breakdown and reassembly of the nuclear envelope. J Cell Sci. 2009; 122:1970–1978. [PubMed: 19494126]

Goldstein JL, DeBose-Boyd RA, Brown MS. Protein sensors for membrane sterols. Cell. 2006; 124:35–46. [PubMed: 16413480]

Horton JD. Sterol regulatory element-binding proteins: transcriptional activators of lipid synthesis. Biochem Soc Trans. 2002; 30:1091–1095. [PubMed: 12440980]

Horton JD, Goldstein JL, Brown MS. SREBPs: activators of the complete program of cholesterol and fatty acid synthesis in the liver. Journal of Clinical Investigation. 2002; 109:1125–1131. [PubMed: 11994399]

Kamath RS, Fraser AG, Dong Y, Poulin G, Durbin R, Gotta M, Kanapin A, Le Bot N, Moreno S, Sohrmann M, et al. Systematic functional analysis of the *Caenorhabditis elegans* genome using RNAi.[see comment]. Nature. 2003; 421:231–237. [PubMed: 12529635]

Lev S. Lipid homoeostasis and Golgi secretory function. Biochem Soc Trans. 2006; 34:363–366. [PubMed: 16709162]

Manifava M, Thuring JW, Lim ZY, Packman L, Holmes AB, Ktistakis NT. Differential binding of traffic-related proteins to phosphatidic acid- or phosphatidylinositol (4,5)- bisphosphate-coupled affinity reagents. J Biol Chem. 2001; 276:8987–8994. [PubMed: 11124268]

Ohba Y, Sakuragi T, Kage-Nakadai E, Tomioka NH, Kono N, Imae R, Inoue A, Aoki J, Ishihara N, Inoue T, et al. Mitochondria-type GPAT is required for mitochondrial fusion. EMBO J. 2013; 32:1265–1279. [PubMed: 23572076]

Osborne TF, Espenshade PJ. Evolutionary conservation and adaptation in the mechanism that regulates SREBP action: what a long, strange tRIP it's been. Genes Dev. 2009; 23:2578–2591. [PubMed: 19933148]

Peterfy M, Phan J, Xu P, Reue K. Lipodystrophy in the fld mouse results from mutation of a new gene encoding a nuclear protein, lipin. Nat Genet. 2001; 27:121–124. [PubMed: 11138012]

Peterson TR, Sengupta SS, Harris TE, Carmack AE, Kang SA, Balderas E, Guertin DA, Madden KL, Carpenter AE, Finck BN, et al. mTOR Complex 1 Regulates Lipin 1 Localization to Control the SREBP Pathway. Cell. 2011; 146:408–420. [PubMed: 21816276]

Quilty D, Gray F, Summerfeldt N, Cassel D, Melancon P. Arf activation at the Golgi is modulated by feed-forward stimulation of the exchange factor GBF1. J Cell Sci. 2014; 127:354–364. [PubMed: 24213530]

Randazzo PA, Kahn RA. GTP hydrolysis by ADP-ribosylation factor is dependent on both an ADP-ribosylation factor GTPase-activating protein and acid phospholipids. J Biol Chem. 1994; 269:10758–10763. [PubMed: 8144664]

Reue K. The role of lipin 1 in adipogenesis and lipid metabolism. Novartis Found Symp. 2007; 286:58–68. discussion 68–71, 162–163, 196–203. [PubMed: 18269174]

Reue K, Zhang P. The lipin protein family: dual roles in lipid biosynthesis and gene expression. FEBS Lett. 2008; 582:90–96. [PubMed: 18023282]

Rual JF, Ceron J, Koreth J, Hao T, Nicot AS, Hirozane-Kishikawa T, Vandenhaute J, Orkin SH, Hill DE, van den Heuvel S, et al. Toward improving *Caenorhabditis elegans* phenome mapping with an ORFeome-based RNAi library. Genome Res. 2004; 14:2162–2168. [PubMed: 15489339]

Sarri E, Sicart A, Lazaro-Dieguez F, Egea G. Phospholipid synthesis participates in the regulation of diacylglycerol required for membrane trafficking at the Golgi complex. J Biol Chem. 2011; 286:28632–28643. [PubMed: 21700701]

Spang A. ARF1 regulatory factors and COPI vesicle formation. Current opinion in cell biology. 2002; 14:423–427. [PubMed: 12383792]

Takeuchi K, Reue K. Biochemistry, physiology, and genetics of GPAT, AGPAT, and lipin enzymes in triglyceride synthesis. American journal of physiology Endocrinology and metabolism. 2009; 296:E1195–E1209. [PubMed: 19336658]

Vance DE. Phospholipid methylation in mammals: from biochemistry to physiological function. Biochimica et biophysica acta. 2014; 1838:1477–1487. [PubMed: 24184426]

Walker AK, Jacobs RL, Watts JL, Rottiers V, Jiang K, Finnegan DM, Shioda T, Hansen M, Yang F, Niebergall LJ, et al. A conserved SREBP-1/phosphatidylcholine feedback circuit regulates lipogenesis in metazoans. Cell. 2011; 147:840–852. [PubMed: 22035958]

Walker AK, Yang F, Jiang K, Ji J-Y, Watts JL, Purushotham A, Boss O, Hirsch ML, Ribich S, Smith JJ, et al. Conserved role of SIRT1 orthologs in fasting-dependent inhibition of the lipid/cholesterol regulator SREBP. Genes & development. 2010; 24:1403–1417. [PubMed: 20595232]

Wilfling F, Thiam AR, Olarte MJ, Wang J, Beck R, Gould TJ, Allgeyer ES, Pincet F, Bewersdorf J, Farese RV Jr, et al. Arf1/COPI machinery acts directly on lipid droplets and enables their connection to the ER for protein targeting. eLife. 2014; 3:e01607. [PubMed: 24497546]

Yang F, Vought BW, Satterlee JS, Walker AK, Jim Sun Z-Y, Watts JL, DeBeaumont R, Saito RM, Hyberts SG, Yang S, et al. An ARC/Mediator subunit required for SREBP control of cholesterol and lipid homeostasis. Nature. 2006; 442:700–704. [PubMed: 16799563]

Zhang C, Wendel AA, Keogh MR, Harris TE, Chen J, Coleman RA. Glycerolipid signals alter mTOR complex 2 (mTORC2) to diminish insulin signaling. Proc Natl Acad Sci U S A. 2012; 109:1667–1672. [PubMed: 22307628]

Zhang Y, Zou X, Ding Y, Wang H, Wu X, Liang B. Comparative genomics and functional study of lipid metabolic genes in Caenorhabditis elegans. BMC Genomics. 2013; 14:164. [PubMed: 23496871]

Higlights

- A *C. elegans* screen finds *lpin-1* and *arf-1.2* as necessary for low-PC SBP-1 activation.
- Depletion of mammalian *LPIN1* and *ARF1* activates SREBP-1 and rescues low-PC effects.
- Levels of active ARF fall when PC synthesis is blocked or *LPIN1* is depleted.
- Blocking PC synthesis or *LPIN1* siRNA decreases GBF1 association with microsomes.

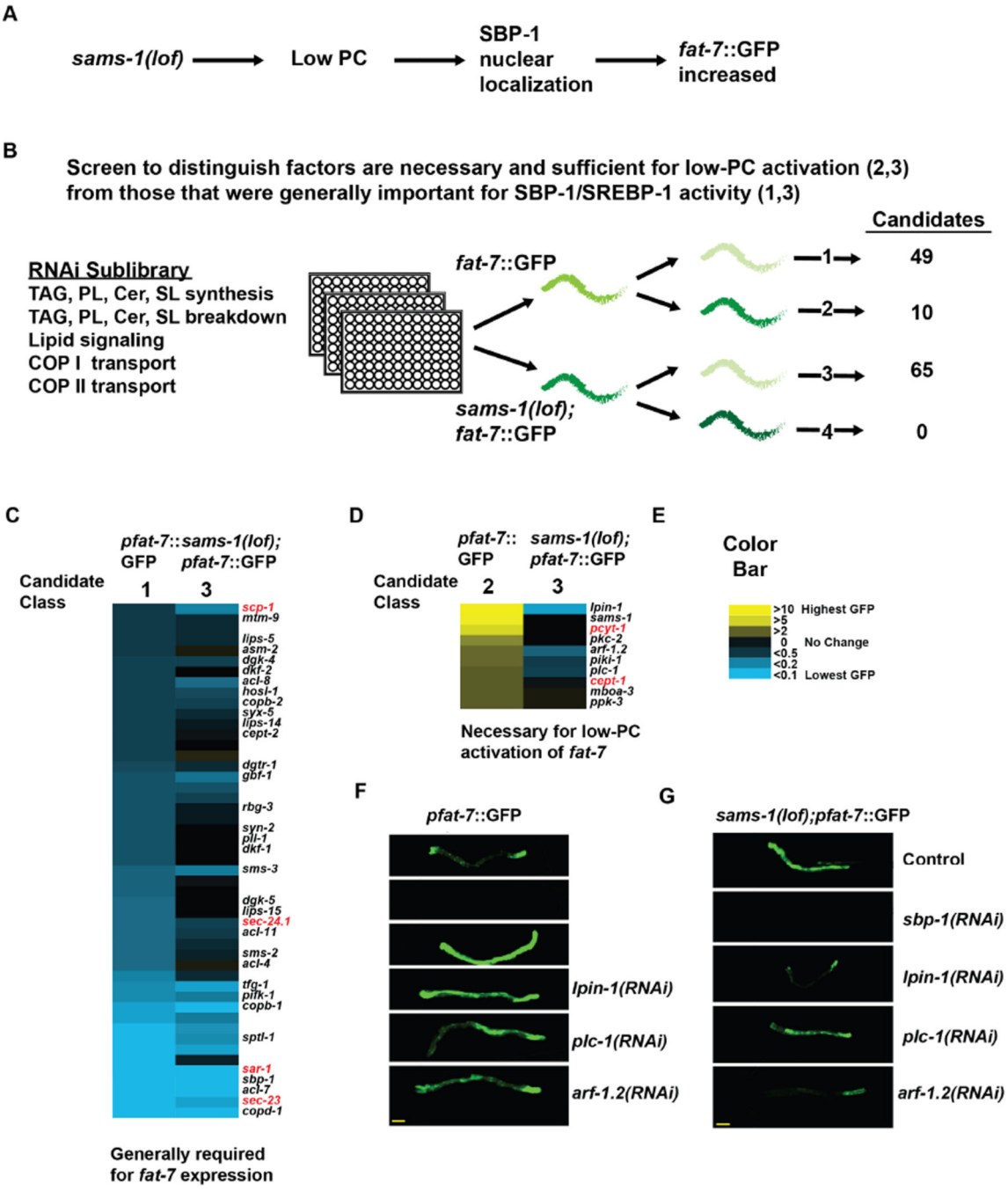

Figure 1. Targeted RNAi screen to identify modulators of SBP-1/SREBP-1 activation in low PC conditions in *C. elegans*

(**A**) Schematic representation of low-phosphatidylcholine (PC) based SBP-1/SREBP-1 activation in *C. elegans*. (**B**) Schematic representation of RNAi screen designed to distinguish factors necessary and sufficient for low-PC based SBP-1 activation (Classes 2,3) from those generally required for SBP-1 function (Classes 1,3). (**C**) Heat map showing genes which down regulate *fat-7* expression in both *pfat-7*::GFP and *sams-1(lof);pfat-7*::GFP animals. (**D**) Heat map showing genes increasing *fat-7* expression in *pfat-7*::GFP animals,

while reducing GFP expression in *sams-1(lof);pfat-7*::GFP animals. (**E**) Color bar representing averaged GFP scores represented by yellow (high) and by blue (low). Epifluorescence imaging showing RNAi of Class 2/3 candidates in *pfat-7*::GFP (**F**) or *sams-1(lof);pfat-7*::GFP (**G**) in young adult *C. elegans*. Scale bar show 75 microns. See also, Table S1, Figure S1.

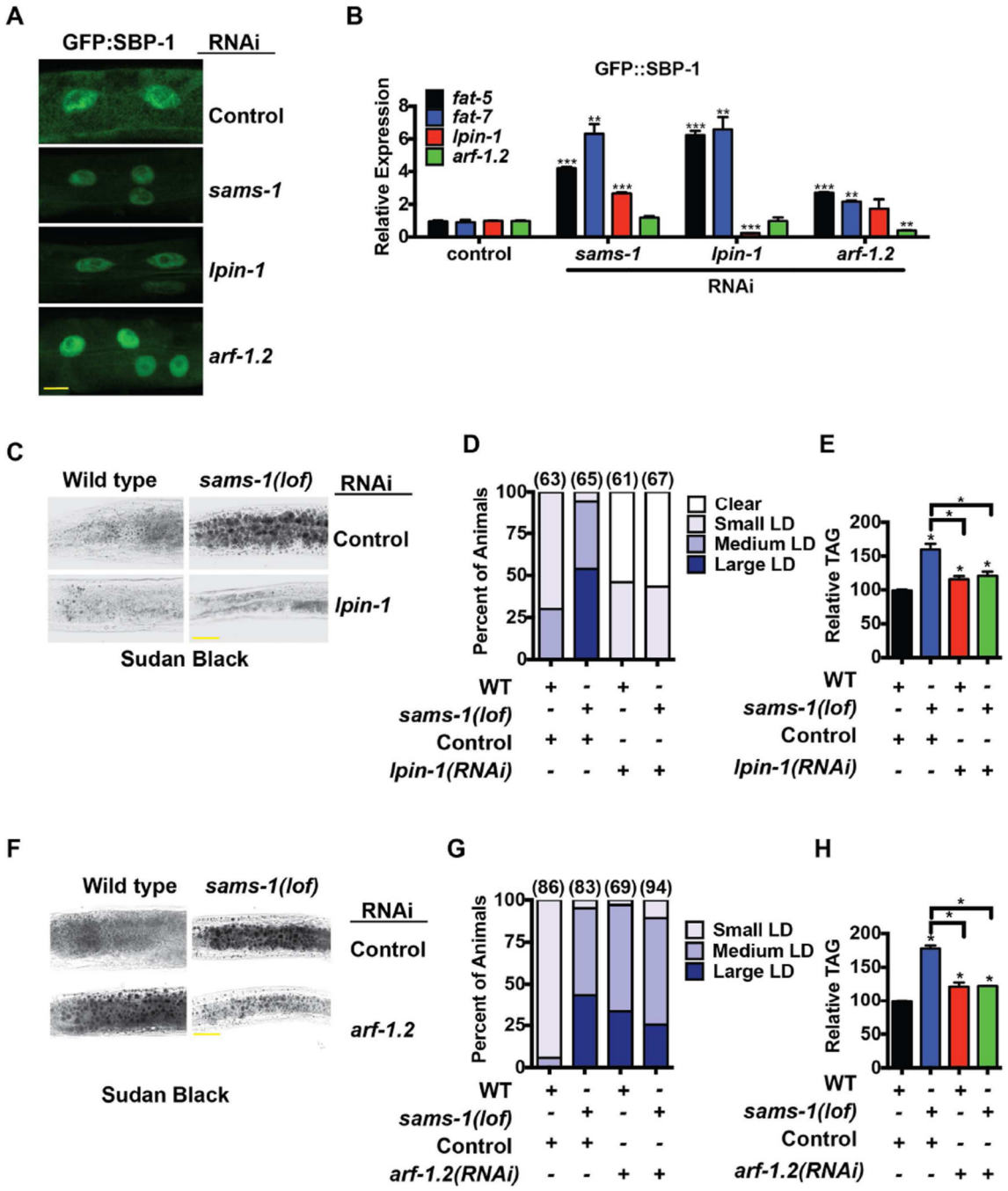

Figure 2. In *C. elegans*, *lpin-1* and *arf-1.2* RNAi increase nuclear localization of SBP-1::GFP and are important for lipid accumulation in *sams-1(lof)* animals

(**A**) Confocal projection showing nuclear accumulation of intestinal GFP::SBP-1 after *sams-1, lpin-1* or *arf-1.2* RNAi. Scale bar for shows 10 microns. (**B**) Quantitative RT-PCR (qRT-PCR) showing upregulation of *fat-5* and *fat-7*. Lipid accumulation when *sams-1* and *lpin-1* where co-depleted assessed by Sudan Black staining (**C**) with quantitation of percent of animals stained (**D**) or TAG level (**E**). Scale bar for Sudan Black shows 25 microns. For *sams-1* and *arf-1.2* co-depletion, Sudan Black staining and quantitation are in (**F, G)** and

TAG measurements in (**H)**. Number of animals is shown in parentheses. Error bars show standard deviation. Results from student's T test shown by *p<0.05, **p<0.01, ***p<0.005. See also Table S2, Figure S2.

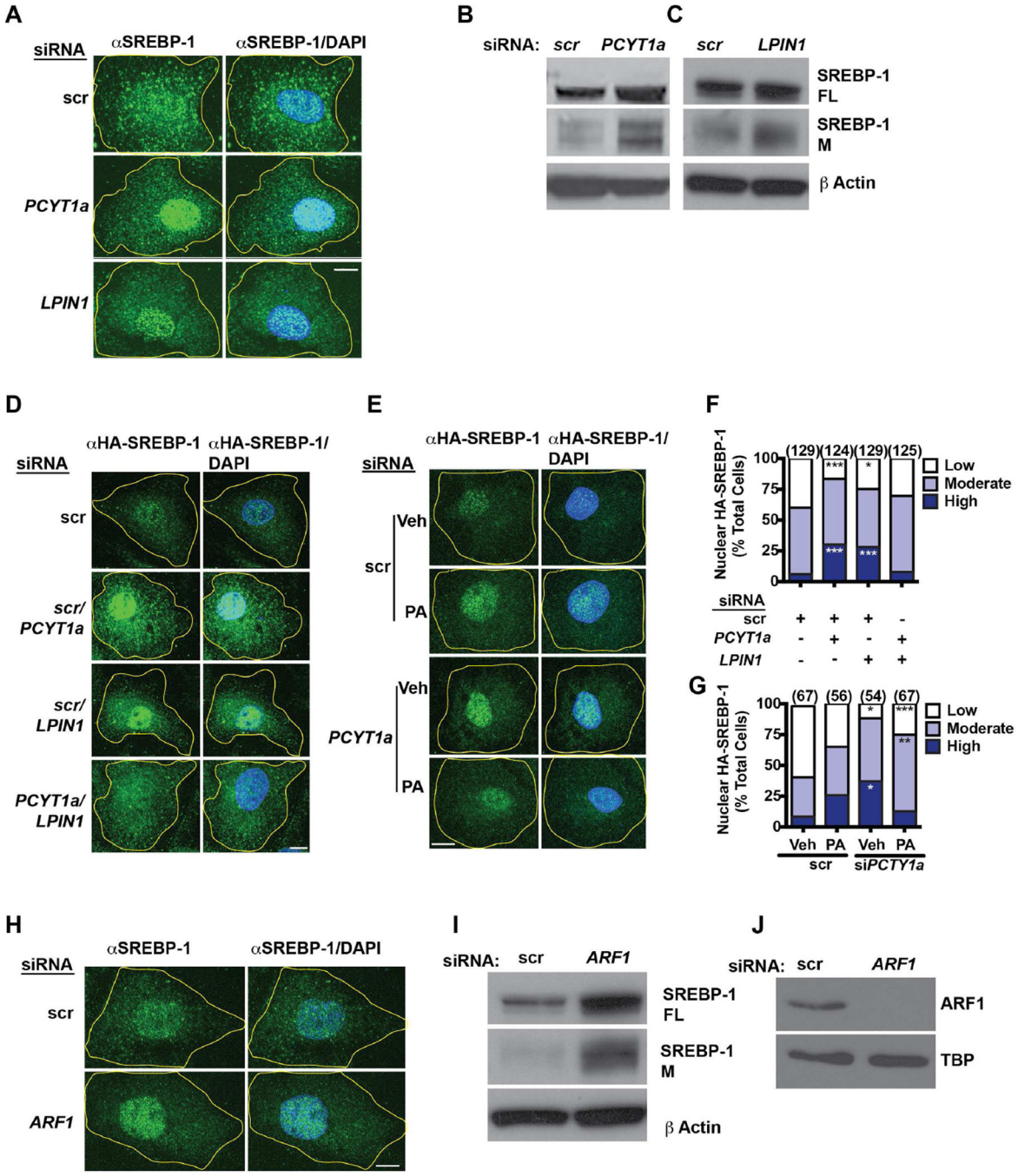

Figure 3. siRNA knockdown of *LPIN1* is similar to *PCYT1* depletion, increasing SREBP-1 nuclear accumulation in human cells

Confocal projections of immunostaining of endogenous SREBP-1 (**A**) or immunoblots (**B, C**) showing accumulation of the nuclear, processed form after siRNA of *PCYT1a* or *LPIN1* in HepG2 cells. scr is the scrambled siRNA control and yellow lines show cell boundaries. FL shows the full length SREBP-1 precursor and M is the mature, cleaved version. (**D**) Confocal projections of HA-SREBP-1 levels after double knockdown of *PCYT1* and *LPIN1* in HepG2 cells with quantitation in (**F**). (**E**) Immunostaining and confocal projection of

HepG2 cells shows increased nuclear accumulation of HA-SREBP-1 in cells treated with phosphatidic acid (PA). PA treatment decreases nuclear HA-SREBP-1 in si*PCYT1a* knockdown cells. Quantitation is in (**G)**. Endogenous SREBP-1 localization is shown by confocal projections of immunostaining (**H**) or by immunoblot (**I**) after treatment of HepG2 cells with siRNA to *ARF1*. scr is scrambled control and yellow lines show cell outlines. (**J**) Immunoblots show decrease in ARF1 after siRNA treatment. Number of cells are shown in parenthesis. Results from student's T test shown by *p<0.05, **p<0.01, ***p<0.005. Scale bars show 10 microns. See also Table S3, Figure S4, 5.

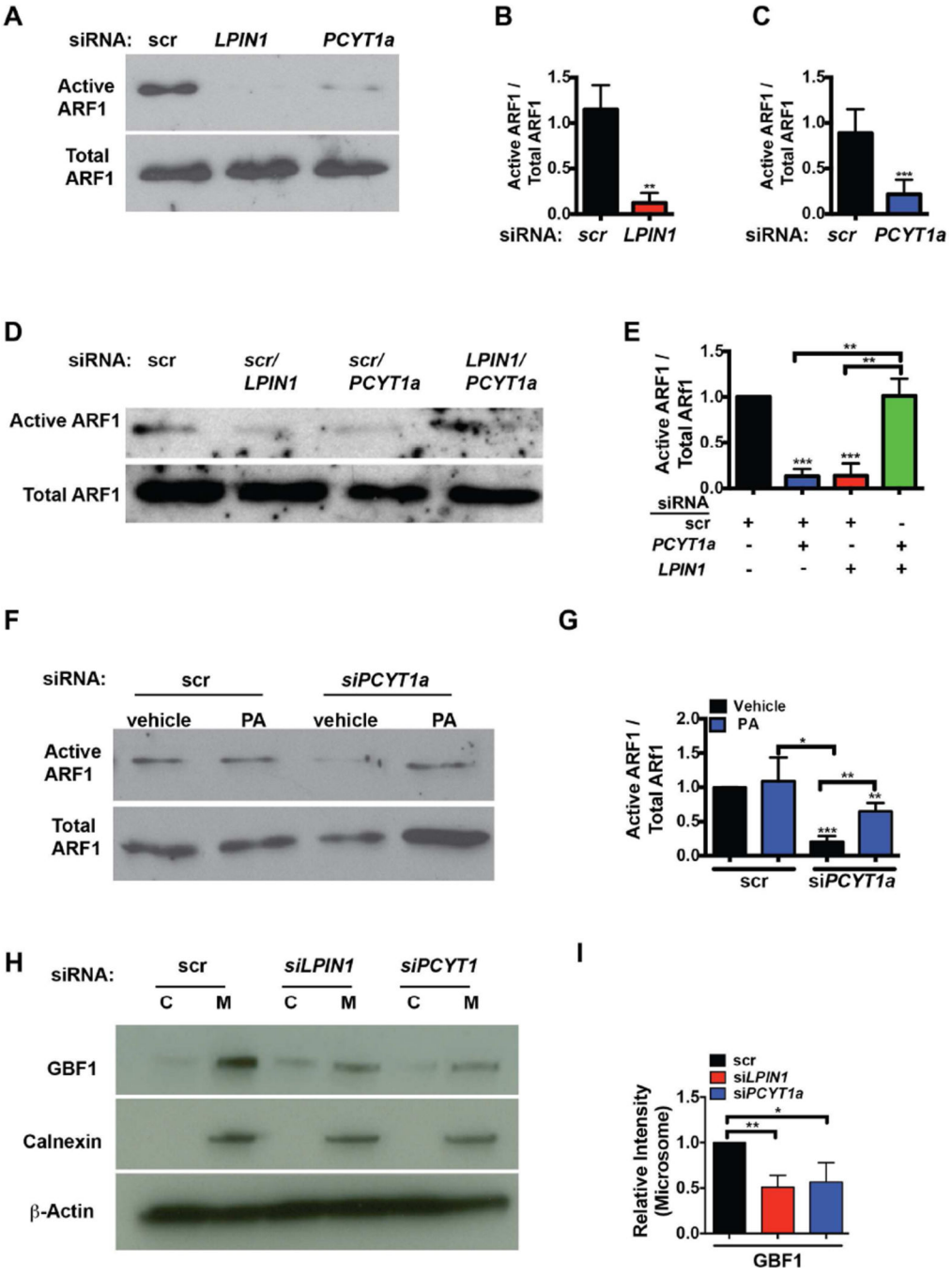

Figure 4. Knockdown of mammalian *PCTY1* or *LPIN1* decreases ARF1 activity

(**A**) Pulldown assays specific for GTP-bound ARF1 show significant decreases after *LPIN1* or *PCTY1a* knockdown. Densitometry showing an average of 3 experiments for *siLPIN1* or 5 experiments for *siPCTY1a* is shown in (**B**) and (**C**) respectively. Comparison of active ARF1 levels shown in a representative immunoblot (**D**) or by densitometry from immunoblots of the double knockdown of *PCYT1a* and *LPIN1* (**E**). Assessment of active ARF1 levels after *PCYT1a* siRNA or treatment with PA shown by immunblot (**F**) or by densitometry (**G**). (**H**) Immunoblots of fractionated HepG2 cells comparing cytosolic (C) to

microsomal (M) association of GBF1 or ARF1 after knockdown of *PCYT1a* or *LPIN1*. Calnexin shows membrane-associated fractions and β-actin confirms loading. For densitometry, values were normalized to vehicle treated scrambled (scr) expressing cells and represent three independent experiments. Error bars show standard deviation. Results from student's T test shown by *p<0.05, **p<0.01, ***p<0.005 compared to scrambled (scr) conditions. ns is "not-significant".